



Universiteit
Leiden
The Netherlands

Solvent tolerance mechanisms in *Pseudomonas putida*

Kusumawardhani, H.

Citation

Kusumawardhani, H. (2021, March 11). *Solvent tolerance mechanisms in Pseudomonas putida*. Retrieved from <https://hdl.handle.net/1887/3151637>

Version: Publisher's Version

License: [Licence agreement concerning inclusion of doctoral thesis in the Institutional Repository of the University of Leiden](#)

Downloaded from: <https://hdl.handle.net/1887/3151637>

Note: To cite this publication please use the final published version (if applicable).

Cover Page



Universiteit Leiden



The handle <https://hdl.handle.net/1887/3151637> holds various files of this Leiden University dissertation.

Author: Kusumawardhani, H.

Title: Solvent tolerance mechanisms in *Pseudomonas putida*

Issue Date: 2021-03-11

CHAPTER 5

Adaptive laboratory evolution restores solvent tolerance in plasmid-cured *Pseudomonas putida* S12; a molecular analysis

Hadiastri Kusumawardhani, Benjamin Furtwängler, Matthijs Blommestijn, Adèle Kaltenytė, Jaap van der Poel, Jan Kolk, Rohola Hosseini, Johannes H. de Winde

Submitted for publication.

DOI: 10.1101/2020.08.01.232264

Abstract

Pseudomonas putida S12 is intrinsically solvent-tolerant and constitutes a promising platform for biobased production of aromatic compounds and biopolymers. The genome of *P. putida* S12 consists of a 5.8 Mbp chromosome, and a 580 kbp megaplasmid pTTS12 that carries several gene clusters involved in solvent tolerance. Removal of pTTS12 caused a significant reduction in solvent tolerance. In this study, we succeeded in restoring solvent tolerance in plasmid-cured *P. putida* S12 using adaptive laboratory evolution (ALE), underscoring the innate solvent-tolerance of this strain.

Whole genome sequencing revealed several single nucleotide polymorphisms (SNPs) and a mobile element insertion, enabling ALE-derived strains to survive and sustain growth in the presence of a high toluene concentration (10% (vol/vol)). Mutations were identified in an RND efflux pump regulator *arpR*, resulting in constitutive upregulation of the multifunctional efflux pump ArpABC. SNPs were also found in the intergenic region and subunits of ATP synthase, RNA polymerase subunit β' , global two-component regulatory system (GacA/GacS) and a putative AraC-family transcriptional regulator Afr. RNA-seq analysis further revealed a constitutive down-regulation of energy consuming activities in ALE-derived strains, including flagellar assembly, F₀F₁ ATP synthase, and membrane transport proteins. Our results indicate that constitutive expression of an alternative solvent extrusion pump in combination with high metabolic flexibility ensures restoration of solvent-tolerance in *P. putida* S12 lacking its megaplasmid.

Introduction

Pseudomonas putida is a promising microbial host for biobased production of valuable chemicals and biopolymer compounds (1). Endowed with its natural versatility, *P. putida* is robust towards toxic compounds which may arise in whole-cell biocatalysis processes as substrates, intermediates, or products. *P. putida* displays a remarkable intrinsic oxidative stress- and solvent-tolerance. This may be further optimized for utilization of secondary feedstock as carbon source and production of various aromatic compounds and bioplastics monomers (2–9). Moreover, several metabolic models and genetic tools are currently available for the design and implementation of novel biosynthetic pathways in *P. putida* (10–12).

P. putida S12 was isolated from soil on minimal media to use styrene as its sole carbon source (13). It is highly tolerant towards organic solvents and aromatic compounds which are often toxic towards microbial hosts. As such, this strain has been used to produce a variety of high value aromatic compounds (6, 8, 9, 14). Organic solvents and aromatic compounds are toxic to most bacteria as these compounds are able to accumulate in the bacterial membrane and thus alter membrane integrity (15), resulting in damage and loss of various membrane functions such as permeability barrier, matrix for protein and metabolic reaction, energy transduction and denaturation of essential enzymes.

The *P. putida* S12 genome comprises of a 5.8 Mbp chromosome and a single-copy 583 kbp megaplasmid pTTS12 (16). Plasmid pTTS12 encodes, among others, an RND efflux pump (SrpABC), a styrene–phenylacetate degradation pathway, and a toxin-antitoxin module *slvTA* are responsible for high solvent tolerance of *P. putida* S12 (13, 17, 18). A significant reduction of solvent-tolerance was previously demonstrated when *P. putida* S12 was cured from its megaplasmid. As a result of plasmid-curing, *P. putida* S12 Δ pTTS12 could only survive and sustain growth in a maximum of 0.15% (vol/vol) toluene (18). As a comparison, wildtype S12 can sustain growth in 0.30% toluene and survive up to 10% toluene. However, as was previously demonstrated, the expression of SrpABC efflux pump in *E. coli* and the non-solvent-tolerant *P. putida* KT2440 instigated still a lower solvent-tolerance than in *P. putida* S12, indicating the intrinsic solvent-tolerance of *P. putida* S12 (18).

In this paper, we further addressed the intrinsic solvent tolerance of *P. putida* S12. Megaplasmid pTTS12 may confer genetic adaptation towards environmental chemical stressors like organic solvents and aromatic compounds, through horizontal gene transfer. Here, we examined the ability of plasmid-cured *P. putida* S12 to survive and sustain growth in the

presence of toluene. Using adaptive laboratory evolution (ALE), we were able to restore the solvent tolerance in *P. putida* S12 lacking the megaplasmid. Specific mutations putatively responsible for the restored solvent-tolerance trait were characterized. Moreover, RNA-seq transcriptional analysis revealed the constitutive responses of the plasmid-cured *P. putida* S12 after adaptation to the elevated toluene concentration.

Materials and Methods

Strains and culture conditions

Strains and plasmids used in this paper are listed in Table 5.S1. *P. putida* strains were grown in Lysogeny Broth (LB) on 30 °C with 200 rpm shaking. *E. coli* strains were cultivated in LB on 37 °C with 250 rpm. For solid cultivation, 1.5 % (wt/vol) agar was added to LB. When required, gentamycin (25 mg l⁻¹), ampicillin (100 mg l⁻¹), kanamycin (50 mg l⁻¹), and streptomycin (50 mg l⁻¹) were added to the media. Hartman's minimal medium (13) was supplemented with 2 mg MgSO₄ and 0.2 % (wt/vol) of citrate, 0.4% (wt/vol) of glycerol, or 0.2% (wt/vol) of glucose may be added as sole carbon source. Growth parameters were measured in a 96-well plates using a Tecan Spark 10M instrument and calculated using growthcurver R-package ver.0.3.0 (19). Maximum growth rate (μ_{max}) was calculated as the fastest growth rate when there were no restrictions imposed on total population size ($t = 2-5$ hours). Maximum OD₆₀₀ (maxOD) was defined as the OD₆₀₀ measurement after the stationary phase was reached ($t \sim 10$ hours). Solvent tolerance analysis was performed by growing 20 ml of *P. putida* culture (starting OD₆₀₀ ± 0.1) on LB with the addition of toluene (0.15 – 10% (vol/vol) in 250 ml Boston glass bottles with Mininert® valve (Sigma-Aldrich) bottle caps. Cell turbidity (OD600) was measured at timepoint 0, 4, 24, and 48 hours to indicate biomass growth. If biomass growth could not be observed, 1 ml of the liquid culture was plated with serial dilution to determine the bacterial survival (viable cell count).

Adaptive Laboratory Evolution

P. putida strains were grown overnight on LB, 30 °C with 200 rpm shaking. Starting cultures were diluted 100 times with LB (starting OD₆₀₀ ± 0.05) and 20 ml of this diluted cultures were placed in Boston bottles. Toluene was added (0.15% (vol/vol)) into the cultures and the bottles were immediately closed using Mininert® bottle caps. These cultures were grown on 30 °C with 200 rpm shaking for approximately 24-48 hours to allow the strains to reach stationary

phase. The toluene-adapted cultures were then diluted 100 times with LB and grown overnight on 30 °C with 200 rpm shaking. Stocks were made from this LB culture and the cycle of toluene adaptation were continued with higher toluene concentration (0.2% (vol/vol)). This cycle was repeated up to 8 cycles with the addition of 0.5% (vol/vol) toluene as shown on Fig. 5.1A.

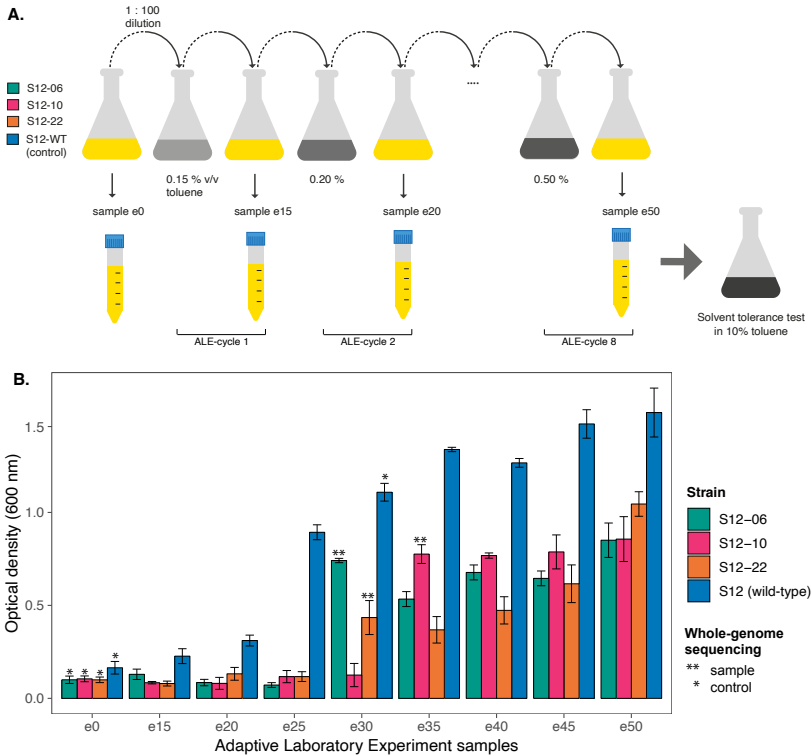


Fig. 5.1. Adaptive laboratory evolution (ALE) experiment of the plasmid-cured *P. putida* S12 to increasing concentration of toluene

- Experimental design of ALE. ALE was performed on three plasmid-cured *P. putida* S12 strains (S12-06, S12-10, and S12-11). In the ALE experiment, LB media (yellow) was used as the growth media with the addition of increasing toluene concentration 0.05% (vol/vol) every cycle (grey).
- Plasmid-cured *P. putida* S12 regained the ability to grow on high toluene concentration. The solvent-tolerance phenotype of ALE-derived strains was tested by observing strain growth on LB with 10% (vol/vol) toluene within 48 hours. The asterisks (*) and double asterisk (**) indicate the control and sample strains that were taken for whole genome sequencing. This experiment was performed with three biological replicates and error bars indicate standard deviation.

PCR and cloning methods

PCR reactions were performed using Phusion polymerase (Thermo Fisher) according to the manufacturer's manual. Oligos used in this paper (Table 5.S2) were procured from Sigma-Aldrich. PCR products were analysed by gel electrophoresis on 1 % (wt/vol) TBE agarose containing 5 $\mu\text{g mL}^{-1}$ ethidium bromide (110V, 0.5x TBE running buffer).

Deletion of *arpR*, *gacA*, *gacS*, and *afr* genes and restoration of mutations on ALE-derived strains were performed using homologous recombination between free-ended DNA sequences that are generated by cleavage on unique I-SceI sites (20). Two homologous recombination fragments (TS-1 and TS-2) were obtained by performing PCR using oligos listed in Table 5.S2. Reverse engineering of the point mutations at ATP synthase subunit α (RPPX_09510) and RNA polymerase subunit β' (RPPX_06985) loci were performed using CRISPR-cas9 enhanced single stranded DNA (ssDNA) recombineering method (21, 22). Spacers and ssDNA repair fragments were created using oligos listed in Table 5.S2. All of the obtained plasmid constructs, deletion, and restoration of the selected genes were verified by Sanger sequencing (Macrogen BV., Amsterdam).

Whole-genome sequencing of plasmid-cured and ALE-derived strains

For whole genome sequencing, DNA was extracted by phenol-chloroform extraction followed by column clean-up using NucleoSpin® DNA Plant II kit (Macherey-Nagel). Clustering and DNA sequencing of wildtype, plasmid-cured, and ALE-derived *P. putida* S12 strains were performed using Illumina cBot and HiSeq 4000 (GenomeScan BV, The Netherlands). Image analysis, base calling, and quality check were performed with the Illumina data analysis pipeline RTA v.2.7.7 and Bcl2fastq v.2.17. Raw-data reads were assembled according to the existing complete genome sequence (Accession no. CP009974 and CP009975) in Geneious software (16).

RNA sequencing of plasmid-cured and ALE-derived strains

Wildtype, plasmid-cured, and ALE-derived *P. putida* S12 cultures were grown from overnight culture (100 times diluted) on 20 ml LB for 2 hours (30 °C, 200rpm) with and without the addition of 0.1% (vol/vol) toluene to bacterial cell cultures. RNA was extracted using TRIzol reagent (Invitrogen) according to the manufacturer's manual. The obtained RNA samples were cleaned-up using NucleoSpin® RNA Plant and Fungi kit (Macherey-Nagel). RNA libraries

were prepared for sequencing using standard Illumina protocols and paired-end sequence reads were generated using the Illumina MiSeq system (BaseClear BV, The Netherlands). Initial quality assessment was based on data passing the Illumina Chastity filtering. Subsequently, reads containing PhiX control signal were removed using an in-house filtering protocol. In addition, reads containing (partial) adapters were clipped (up to a minimum read length of 50 bp). The second quality assessment was based on the remaining reads using the FASTQC quality control tool version 0.11.5. Tophat2 version 2.1.1 aligned RNA-seq reads to a reference genome (Acc. No. CP009974 and CP009975) using the ultra-high-throughput short read aligner Bowtie version 2.2.6 (23, 24). Cufflink was used to test for differential expression and regulation in RNA-Seq samples. Cuffdiff then estimated the relative abundances of these transcripts.

Microtiter dish biofilm formation assay

To quantify biofilm formation, crystal-violet based assay on 96-well plate was performed as described by O'Toole (25). Overnight cultures of *P. putida* S12 (100 times diluted) were grown in flat bottomed 96-well microtiter plate with 100 μ l LB media (30 °C) for 6 hours without shaking. After 6 hours, OD₆₀₀ was measured using Tecan Spark® 10M (Tecan) to ensure the growth of *P. putida* S12. Liquid cultures were removed from 96-well microtiter plate and followed by two-times washing with water. Crystal violet solution (0.1% (vol/vol)) 125 μ l was added to each well followed by 10-15 minutes of incubation. After incubation, crystal violet solution was removed and the wells were washed with water to remove the excess crystal violet. Microtiter plate was then turned upside-down and dried. Acetic acid solution (30% (vol/vol)) 125 μ l were added to solubilized biofilm stained crystal violet and incubated for 10-15 minutes. The absorbance at 550 nm was measured to represent biofilm formation using Tecan Spark® 10M (Tecan) and acetic acid solution as blank.

Swimming motility assay

As starting culture, *P. putida* S12 strains were streaked and grown on LB agar overnight (30 °C). Single colonies were picked and stab-inoculated on to low viscosity LB agar (0.3% (wt/vol) agar). This agar was incubated cap-side up for 24 hours at 30 °C. Radial growth of *P. putida* S12 on low-viscosity agar was measured with three replicates to represent swimming motility.

Data availability

Whole genome sequencing data for the wild-type, plasmid-cured genotypes, and ALE-derived *P. putida* S12 have been submitted to the SRA database under accession number PRJNA602416. Datasets generated from RNA-seq experiment have been submitted to the GEO database under accession number GSE144045.

Results

Plasmid-cured *Pseudomonas putida* S12 can regain the ability to tolerate high-concentration toluene

To investigate the intrinsic solvent-tolerance of *P. putida* S12, we performed adaptive laboratory evolution (ALE) experiment on plasmid-cured *P. putida* S12. Three biological replicates of plasmid-cured *P. putida* S12 (strain S12-06, S12-10, and S12-22) and a wildtype *P. putida* S12 as control were set up to grow on lysogeny broth (LB) media with the addition of 0.15% (vol/vol) toluene; the initial maximum concentration that can be tolerated by plasmid-cured *P. putida* S12 (Fig. 5.1A). At stationary phase (typically after 24-48 hours), these cultures were transferred (1:100 dilution) to grow overnight on fresh LB media. Overnight LB media cultures were transferred into LB media containing toluene 0.20% (increase of 0.05% toluene) to continue with the next ALE cycle. While plasmid-cured *P. putida* S12 was unable to grow on LB with 0.20% (vol/vol) toluene directly, after adaptation to LB with 0.15% (vol/vol) toluene these cultures are able to grow on LB with 0.20% (vol/vol) toluene. We repeated this growth cycle with increasing concentration every cycle until plasmid-cured *P. putida* S12 strains were able to grow on LB with 0.50% (vol/vol) toluene (Fig. 5.1A). All samples from every ALE-cycle were collected and tested for their ability to survive 10% (vol/vol) toluene on LB for 48 hours. This concentration was chosen to represent a high toluene concentration which creates a distinct second phase layer in the culture medium.

Initially, the plasmid-cured *P. putida* S12 did not show growth and survival in the presence of 10% toluene, while the wild-type *P. putida* S12 can survive $((2.52 \pm 0.31) \times 10^{-2}$ survival frequency) although it did not show any growth in 10% toluene (Fig. 5.1B). After the adaptation with a moderate toluene concentration (0.30-0.35%), both wild-type and plasmid-cured *P. putida* S12 showed a significant increase in their ability to withstand and sustain growth in 10% toluene. ALE-derived strains S12-06e30, S12-10e35, and S12-22e30 were

able to grow on LB media with 10% (vol/vol) toluene, reaching final OD₆₀₀ of 0.741 ± 0.02 , 0.776 ± 0.08 , and 0.434 ± 0.158 respectively after 48 hours. These three samples were taken for whole genome sequencing to map the occurring mutations important for the solvent-tolerance phenotype. Wildtype *P. putida* S12, S12e30, and the initial plasmid-cured *P. putida* S12 strains were sequenced as controls.

Common mutations were identified in solvent-tolerant strains obtained from ALE

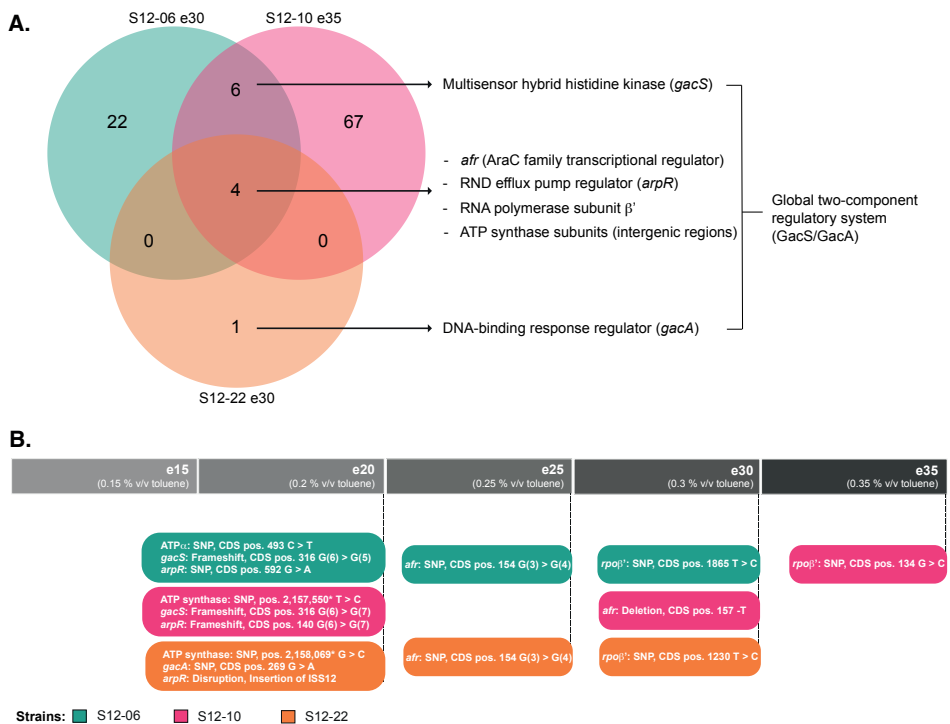


Fig. 5.2. Common mutated loci were identified in the ALE-derived *P. putida* S12 strains.

- Venn diagram of mutated loci in the ALE-derived *P. putida* S12 strains. The colors indicate the three ALE-derived strains. Common mutated loci were identified among ALE-derived strains on an AraC family transcriptional regulator (Afr), RND efflux pump regulator (ArpR), RNA polymerase subunit β' , intergenic region of F0F1 ATP synthase subunits, and global two-component regulatory system GacS/GacA.
- ALE-derived *P. putida* S12 strains accumulated key mutations in a stepwise manner. ALE-derived strains were probed for key mutations accumulation with PCR and Sanger sequencing. The colors indicate the three ALE-derived strains and the grey bar indicate the ALE cycles which the strains were originating from. The position of the occurring SNPs or indels are indicated as CDS position of each mutated loci, except

for the SNPs within the intergenic regions of ATP synthase which positions are indicated relative to the chromosome sequence.

We performed whole genome sequencing of ALE-derived strains S12-06e30, S12-10e35, and S12-22e30 to map the occurring mutations that may lead to increased solvent tolerance in the evolved strains. We identified 32, 77, and 5 mutations (SNPs, insertions/deletions, and mobile element ISS12 insertion) respectively, in S12-06e30, S12-10e35, and S12-22e30 (Fig. 5.2A). Among these mutations, four common mutated loci were identified in all strains. These mutations occurred in an AraC-family transcriptional regulator *Afr* (RPPX_14685), in a RND efflux pump regulator *ArpR* (RPPX_14650), in RNA polymerase subunit β' *rpoB'* (RPPX_06985), and in the intergenic regions and subunits of ATP synthase (RPPX_09480-09510) (Fig. 5.2A). Six mutated loci were shared only between S12-06e30 and S12-10e35. Among these six loci, indels occurred within *gacS* locus (RPPX_15700) in S12-06e30 and S12-10e35 while S12-22e30 had a unique SNP within *gacA* locus (RPPX_00635). In *Pseudomonas*, *GacS* and *GacA* proteins are known to constitute a two-component regulatory system which regulates biofilm formation, cell motility, and secondary metabolism (26).

Since the ALE-derived strains showed a sudden increase in their ability to tolerate high toluene concentrations, we investigated the order of accumulation of key mutations in ALE-derived strains. Key mutations accumulated in a stepwise manner rather than emerging simultaneously in one cycle (Fig. 5.2B). In the second ALE-cycle, three key mutations occurred under the exposure to 0.20% (vol/vol) toluene in all strains (S12-06e20, S12-10e20, and S12-22e20). The first accumulated mutations occurred on the intergenic regions between ATP synthase subunits, *gacS/gacA* loci, and *arpR* locus. In the subsequent cycle, S12-06e25, S12-10e30, and S12-22e25 accumulated additional key mutations in the *afr* locus. The final key mutations on *rpoB'* locus were accumulated by strain S12-06e30, S12-10e35, and S12-22e30, in which the sudden increase of solvent tolerance were observed.

Contribution of key mutations to increased solvent-tolerance of ALE-derived strains

To study the contribution and impact of each mutated locus, single knock-out strains of *arpR* (RPPX_14650), *afr* (RPPX_14685), *gacA* (RPPX_00635), and *gacS* (RPPX_15700) were created in plasmid-cured *P. putida* S12. In the ALE-derived strains, the acquired mu-

tations (indels and mobile element insertion) in *arpR* (RPPX_14650), *afr* (RPPX_14685), and *gacS* (RPPX_15700) caused truncation of the encoded protein, while the SNP in *gacA* (RPPX_00635) caused an amino acid residue change (P90L). The SNPs acquired in ATP synthase and in RNA polymerase subunit β' loci were not addressed with this single knock-out approach since knocking out these genes would have deleterious effects. Solvent-tolerance analysis of the single knock-out strains indicated that deletion of each of those genes improved the growth of plasmid-cured *P. putida* S12 strains on LB with 0.15% (vol/vol) toluene (Fig. 5.3A). However, single knock-out of these genes did not enable plasmid-cured *P. putida* S12 strains to grow on higher toluene concentration than 0.15% (vol/vol).

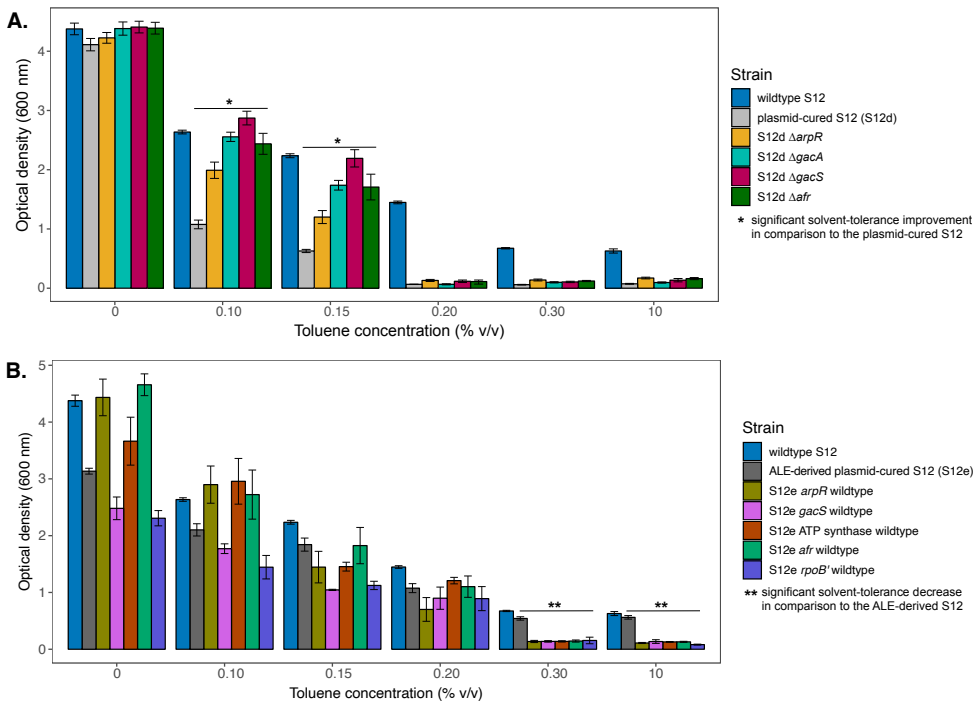


Fig 5.3. Accumulated key mutations contributed to solvent-tolerance phenotype of ALE-derived *P. putida* S12 strains.

- Single-knockout of common mutated loci in the plasmid-cured *P. putida* S12 improved strain growth on LB with low toluene concentration (0.1-0.15% (vol/vol)). The colors indicate the control strains and the plasmid-cured S12 with deleted loci. This experiment was performed with three biological replicates and error bars indicate standard deviation.
- Single-restoration of common mutated loci in the ALE-derived *P. putida* S12 reduced solvent-tolerance phenotype. The colors indicate the control strains and the ALE-derived S12 with restored loci. The restored

strains can grow on LB with a maximum of 0.20% (vol/vol) toluene. This experiment was performed with three biological replicates and error bars indicate standard deviation.

Individual restoration of common mutated loci in the ALE-derived strains to their wild-type sequence caused these strains to lose the ability to withstand the presence of moderate and high toluene concentration (0.30% and 10% (vol/vol) toluene) (Fig. 5.3B). These strains can sustain growth on LB with maximum 0.20% (vol/vol) toluene. Therefore, we concluded that each of the common mutated loci is important for the solvent-tolerance phenotype in ALE-derived strains.

Reverse engineering of key mutations on plasmid-cured S12 successfully restore solvent-tolerance

To confirm the important contribution of key mutations, we introduced these mutations on a plasmid-cured S12 strain and analyse the growth parameters of the resulting strains in the presence and absence of toluene (Fig. 5.4 and Table 5.S3). Strain S12-10 was chosen to represent the plasmid-cured S12 in this experiment. A knock-out of *arpR* (RPPX_14650) locus was performed resulting in the first reverse engineering strain (RE1). Second knock-out mutation at *gacS* (RPPX_15700) locus was performed on strain RE1, resulting in the strain RE2. It is interesting to note that strain RE2 exhibit significantly better growth parameters in LB and minimal media compared to its parent strains RE1 and S12-10 (Table 5.S3). The third mutation was introduced at the ATP synthase subunit alpha (RPPX_09510) to strain RE2, resulting in the strain RE3. This mutation caused an amino acid substitution from arginine to cysteine at position 165 (R165C), mimicking the mutation found in the strain S12-06e30. Indeed, the introduction of this mutation caused a severe reduction of growth parameters in LB and minimal media (Table 5.S3). Fourth knock-out mutation at *afr* (RPPX_14685) locus was performed on strain RE3, resulting in the strain RE4. Finally, a point mutation was introduced to strain RE4 at *rpoB'* (RPPX_06985) locus to construct strain RE5 which caused an amino acid substitution from aspartic acid to glycine at position 622 (D622G) mimicking the mutation found in the strain S12-06e30.

Reverse engineering strains and its parent, strain S12-10, were tested for their ability to survive and sustain growth in the presence of toluene (Fig. 5.4). Strain S12-10, RE1, and RE2 were only able to withstand and sustain growth in the presence of 0.15% (vol/vol) toluene. Nevertheless, strain RE1 and RE2 showed growth improvement in comparison to strain

S12-10 (Fig. 5.4, panel 2). Strain RE3 and RE4 were able to withstand and sustain growth in a slightly higher toluene concentration, 0.20% and 0.25% (vol/vol) toluene respectively. Finally, strain RE5 were able to sustain growth in the presence of high toluene concentration (10% (vol/vol) toluene). These results confirm that the key mutations are indeed important for the restoration of solvent tolerance in plasmid-cured S12.

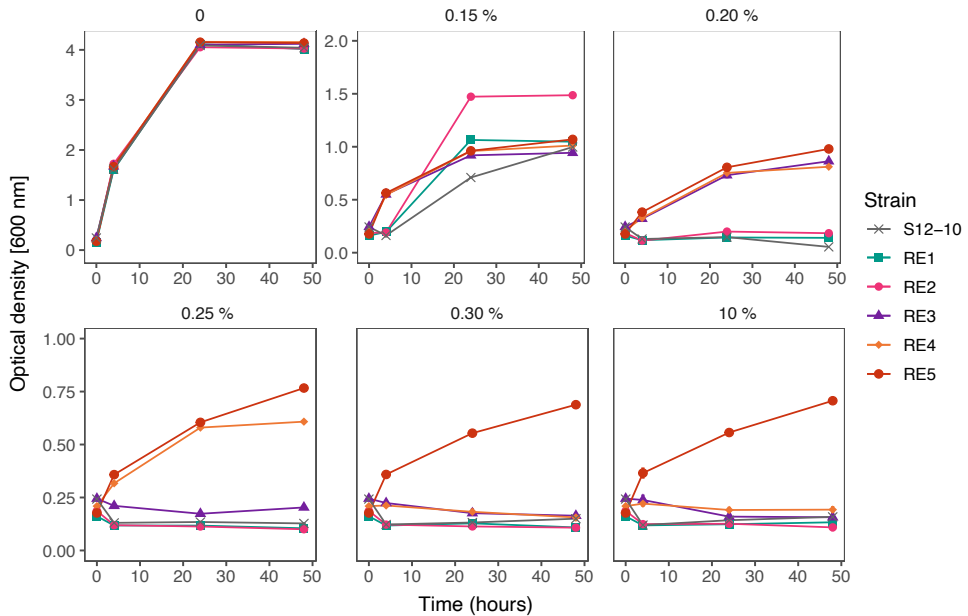


Fig. 5.4. Reverse engineering of the key mutations found in ALE-derived strains

Reverse engineering of the key mutations found in the ALE-derived *P. putida* S12 successfully restores the solvent-tolerance phenotype in the plasmid-cured strain S12-10. The colors indicate the control strain S12-10 and the reverse engineering strains (RE). This experiment was performed with three biological replicates and error bars indicate standard deviation. The y-axis may be different for the presented panels.

Restoration of solvent-tolerance involved a constitutive downregulation of energy consuming activities in ALE-derived strains

Global transcriptional analysis (RNA sequencing) was performed to probe the response of ALE-derived *P. putida* S12 in comparison with wildtype and plasmid-cured *P. putida* S12 in the presence of toluene (LB with 0.1% (vol/vol) toluene). As a response to toluene addition, ALE-derived strains showed differential expression only of 14 loci. This response was in stark contrast to the wild-type S12 and plasmid-cured S12 which differentially expressed more than 500 loci as a response to toluene addition (Fig. 5.S1). Comparisons of gene expression be-

tween ALE-derived strains with plasmid-cured and wildtype *P. putida* S12 growing on LB in the absence of toluene indicated that the mutations which occurred in the ALE-derived strains caused constitutive differential expression of ± 900 genes which play a role in restoring solvent tolerance (Fig. 5.5).

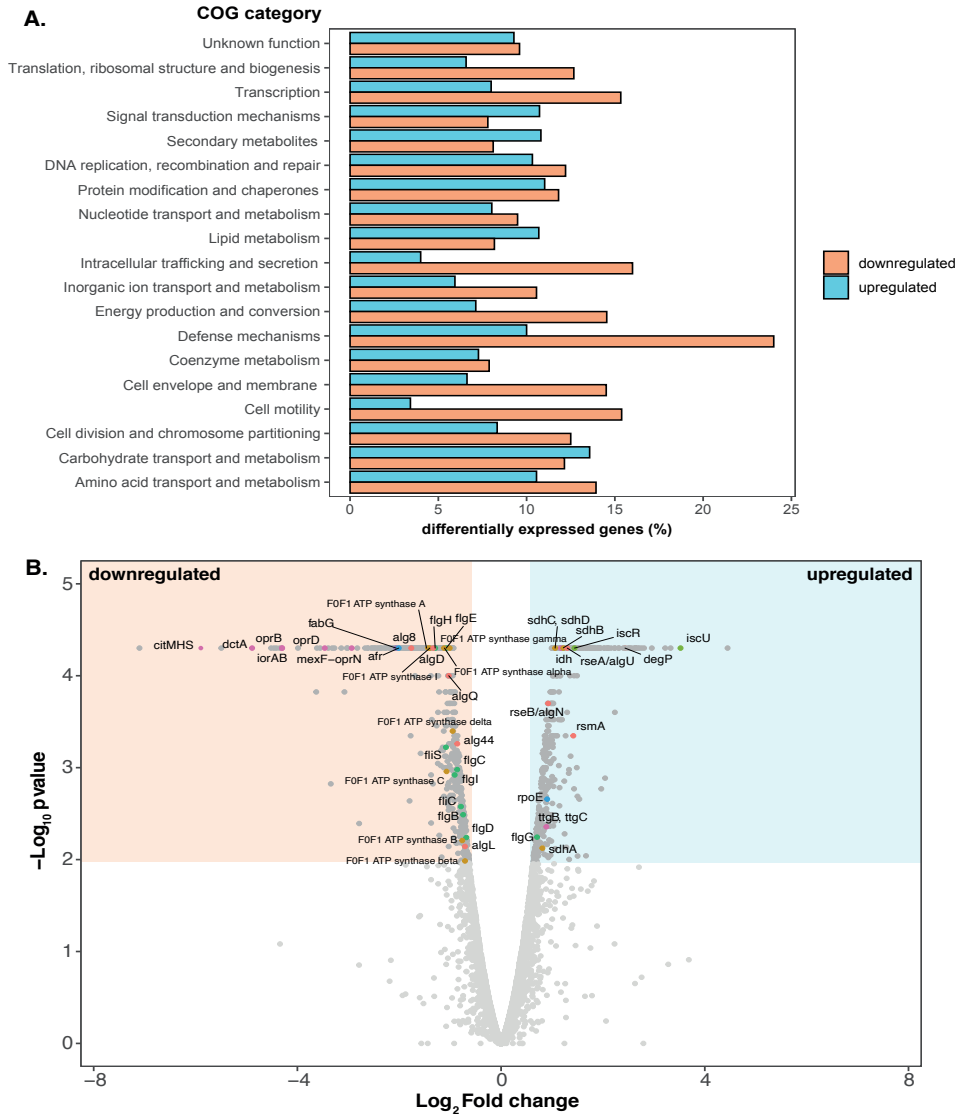


Fig. 5.5. Visualization of differentially expressed genes on ALE-derived *P. putida* S12 strains in comparison to its parental strain growing on LB.

A. COG classification of differential gene expression in ALE-derived strains in comparison to plasmid-cured *P. putida* S12. COG classification was performed using eggNOG 5.0 mapper (<http://eggnogetdb.embl.de/#/app/emapper>). The percentages of up-regulated genes in each class are represented by the blue bar and the

percentages of down-regulated genes are represented by the red bar.

- B. Volcano plot of differential gene expression in ALE-derived strains in comparison to the plasmid-cured *P. putida* S12 growing on LB. Blue area indicates the significantly upregulated genes and beige area indicates the significantly downregulated genes (cut-off: Log_2 Fold Change ≥ 1 for up-regulated genes or ≤ -1 for down-regulated genes and $p\text{-value} \leq 0.01$). The colored dots represent the significantly up/down-regulated genes discussed in this paper. The colors correspond to the functions of each genes: red represents biofilm and alginate production genes; orange represents the genes involved in oxidative phosphorylation process; light green represents the genes involved in energy production process; green represents flagellar assembly gene clusters; blue represents sigma factor and transcriptional regulator; and magenta represents the genes which constitute membrane transporters.

Constitutive differentially expressed genes in ALE-derived strains in comparison to parental plasmid-cured *P. putida* S12 were classified based of COG categorization. Several classes of genes were downregulated in ALE-derived strains compared to plasmid-cured S12, for example, genes constituting cell motility, intracellular trafficking and secretion, and defence mechanism functions (Fig. 5.5A). In general, ALE-derived strains appeared to constitutively shut-down energy consuming activities, such as flagella biosynthesis, F₀F₁ ATP synthase, and membrane transport proteins which are energized through proton (H⁺) influx. Additionally, genes related to biofilm formation were constitutively down-regulated. Here, we focused on several classes of genes that were differentially expressed in ALE-derived strains compared to its parental strain.

Membrane proteins and efflux pumps

ArpABC efflux pump (RPPX_14635-14640) is a multi-functional RND efflux pump homologous to TtgABC from *P. putida* DOT-T1E. This locus was moderately upregulated in ALE-derived strains (Fig. 5.5B; *ttgB* and *ttgC*). While the upregulation of this pump is a common response to toluene in wildtype *P. putida* S12, ALE-derived strains constitutively upregulate ArpABC by SNPs and mobile element insertion in its negative regulator gene *arpR* (RPPX_14650). Interestingly, almost all of the other RND efflux pumps encoded in the chromosome of *P. putida* S12 were downregulated in ALE-derived strains. In the ALE-derived strains, lacking the pTTS12-encoded SrpABC solvent pump, ArpABC is the only remaining efflux pump that may extrude toluene, albeit with a much lower affinity (27). Downregulation of other efflux pumps is likely to be important to preserve the required proton motive force.

The genes associated with porin function were downregulated in ALE-derived strains as exemplified by RPPX_10240, RPPX_14820, and RPPX_17640 which encodes OprD porin

family proteins. This response was similar to previous proteomics study (28) which noted the downregulation of porins to avoid toluene leakage into the cell through these porins. In addition to porins downregulation, several membrane transport proteins like *dctA* (H⁺/C4-dicarboxylate symporters, RPPX_17630) and *citMHS* (citrate-divalent cation/H⁺ symporter, RPPX_17635) were constitutively downregulated.

Energy production and conversion

In ALE-derived strains, F₀F₁ ATP synthase subunits were constitutively downregulated (Fig. 5.5B). This was in-line with our finding of the SNPs which occurred on the intergenic regions between F₀F₁ ATP synthase subunits (RPPX_09480-RPPX_09510). F₀F₁ ATP synthase generates 1 ATP from ADP in bacteria by pumping out 3 H⁺ molecule and thus downregulation of this loci may also contributed to the preservation of proton motive force.

Succinate dehydrogenase (SdhABCD) gene cluster (RPPX_01070-RPPX_01085) were constitutively upregulated in ALE-derived strains. Succinate dehydrogenase is responsible as complex II in oxidative phosphorylation process. Cytochrome C oxidase subunit II (RPPX_08860) and its assembly protein (RPPX_08850), composing complex IV, were also constitutively upregulated in ALE-derived strains. Taken together, these findings underlined the importance of electron transport chain in maintaining proton motive force during solvent-stress.

Biofilm formation

In ALE-derived strains, we observed a constitutive upregulation of the *rsmA* locus (RPPX_02245). Upregulation of *rsmA* locus may be caused by the mutations found in *gacS/gacA* locus and is known to promote motile lifestyle in *Pseudomonas* (26). Downregulation of alginate biosynthesis pathway as the main polysaccharide matrix in *Pseudomonas* biofilm was also observed. Alg44 (RPPX_14155), which upon its interaction with c-di-GMP is known to positively regulate alginate production (29), was constitutively downregulated in ALE-derived strains. Other loci which are involved in alginate biosynthesis and export were also down regulated e.g. *algL* (RPPX_14130), *alg8* (RPPX_14160), *algD* (RPPX_14165), and *algE* (RPPX_21545). Taken together, these findings pointed to reduction of biofilm formation capacity in the ALE-derived strains.

To confirm this result, we applied a microtiter dish biofilm formation assay (25) to assess the biofilm formation in ALE-derived strains (Fig. 5.6A). Biofilm formation was indeed

clearly lower in ALE-derived strains compared to the wildtype and plasmid-cured *P. putida* S12. This tendency was reversed when the indel mutation in the *gacS* locus was restored to the wildtype sequence. While biofilm may protect bacteria from external stressors, nutrient and oxygen depletion during sessile lifestyle may be disadvantageous in solvent-stress and therefore constitutive downregulation of biofilm-related genes was beneficial in ALE-derived strain.

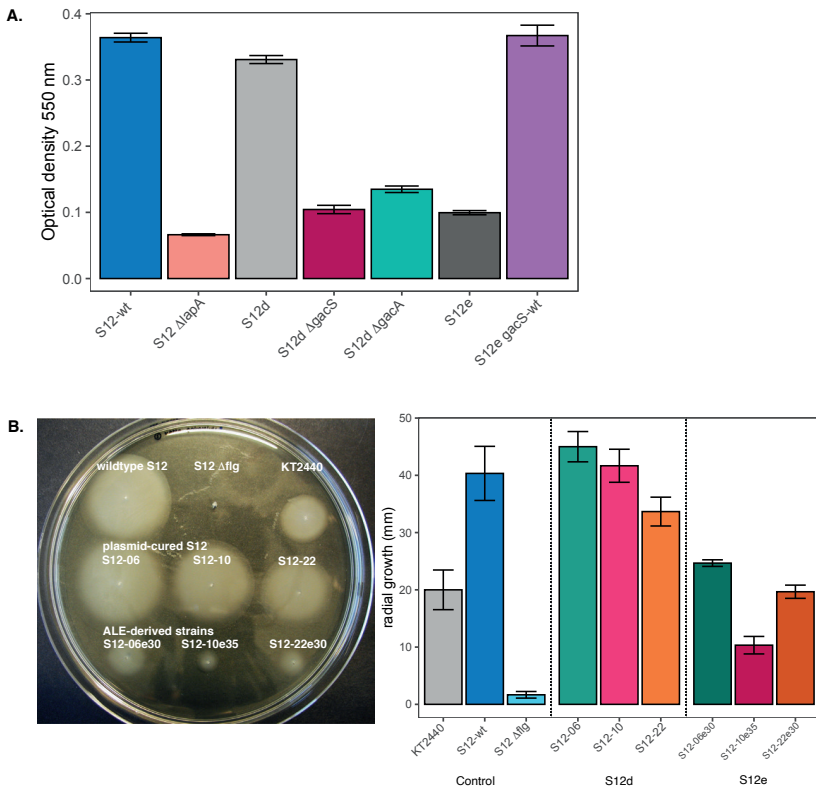


Fig. 5.6. Biofilm formation and cell motility were reduced in ALE-derived *P. putida* S12 strains

- A. Microtiter biofilm formation assay of *P. putida* S12. Plasmid-cured *P. putida* S12 (S12d) Δ *gacS* and Δ *gacA* showed similar reduction as ALE-derived *P. putida* S12 (S12e) strains. Restoration of *gacS* locus to wild-type sequence (S12e *gacS*-wt) also restore biofilm formation in ALE-derived *P. putida* S12 (S12e). The measurement of biofilm formation was performed by measuring optical density at 500nm as previously described (25) with Δ *lapA* (adhesin) taken as negative control. This experiment was performed with three biological replicates and error bars indicate standard deviation.
- B. Swimming motility assay of *P. putida* S12 in low viscosity agar (LB + 0.3% agar). ALE-derived *P. putida* S12 strains (S12e) showed a reduced radial growth in low viscosity agar indicating lower swimming motility.

The *Δflg* (flagella gene cluster) was taken as a negative control. On the second panel, the bars represent an average of radial growth of at least three biological replicates of each strains and error bars indicate standard deviation.

Cell motility

Flagellar biosynthesis loci (RPPX_02045-RPPX_02125) were constitutively downregulated in ALE-derived strains (Fig. 5.5B). Consequently, this may lead to reduced swimming motility in ALE-derived strains. We confirmed this finding by measuring the radial growth of ALE-derived strains in comparison to the wildtype and plasmid-cured *P. putida* S12 on low-viscosity agarose (Fig. 5.6B). Indeed, ALE-derived strains showed a significant reduction of radial growth. Downregulation of flagella may be a strategy of ALE-derived strains to maintain proton motive force and reroute its energy towards extrusion of toluene since both RND efflux pump ArpABC and flagella utilize H⁺ influx as energy source.

Chaperones

We also observed the constitutive upregulation of loci RPPX_14680-14875 which encode homologs of sigma factor E (RpoE), anti-sigma factor RseAB, and DegP protein respectively. This cluster is known to orchestrate the expression of chaperone proteins as a stress response to the elevated amount of misfolded proteins in *E.coli* (30). Additionally, these sigma factors are known to negatively regulate alginate biosynthesis in *P. aeruginosa* (31). Other chaperone protein, like Hsp20 protein (RPPX_17155) was also constitutively upregulated in ALE-derived strains. Constitutive upregulation of these genes suggested an important role of chaperones in the adaptive response to high toluene concentration.

Discussion

Solvent tolerance can be restored in a relatively small number of generations

The single copy megaplasmid pTTS12 plays an essential role in the solvent-tolerance trait of *P. putida* S12. An efficient solvent extrusion pump SrpABC (homologous to TtgGHI), styrene-phenylacetate degradation pathway, and the recently-identified toxin-antitoxin SlvTA are encoded within this megaplasmid (16). Unlike *P. putida* DOT-T1E, *P. putida* S12 does not encode toluene degradation pathway within its genome and thus, its solvent-tolerance heavily relies on the gene clusters encoded in pTTS12 as mentioned above (32). However, previous

attempts expressing SrpABC in other non-solvent tolerance bacteria like *E. coli* were unsuccessful to incite the same level of solvent-tolerance as with *P. putida*. This may indicate that *P. putida* S12 is intrinsically solvent tolerant to begin with (33, 34). Hence, in this paper, we further scrutinized this putative intrinsic solvent tolerance in *P. putida* S12 using Adaptive Laboratory Evolution (ALE).

Upon curing of megaplasmid pTTS12, solvent-tolerance of *P. putida* S12 was significantly reduced. After 4-5 adaptation cycles (± 7 generations per growth cycle) to increasing toluene concentrations, solvent-tolerance trait of plasmid-cured *P. putida* S12 could be restored. Relatively short adaptation to alternating cycles of LB in the presence or absence of toluene can restore solvent-tolerance to elevated concentration of toluene due to the stringent selection pressure elicited by this experimental set-up. However, we also observed a severe reduction in growth parameters on the resulting ALE-derived strains grown in the absence of toluene compared to wildtype *P. putida* S12 undergoing the same adaptation cycles to toluene. Several common mutated loci were identified between replicates of ALE-derived *P. putida* S12. Whole genome sequencing revealed SNPs, indels, and an insertion of mobile genetic element ISS12 occurred in a negative regulator of RND efflux pump ArpR, an uncharacterized AraC family transcriptional regulator Afr, RNA polymerase subunit β' , intergenic region of F0F1 ATP synthase subunits and global two-components regulatory system GacS/GacA. Each of these mutations were demonstrated to be essential in restoring solvent-tolerance of the plasmid-cured *P. putida* S12.

Up-regulation of solvent efflux pump is compensated by down-regulation of other membrane proteins

RNA-sequencing revealed constitutive differential changes of gene expression in ALE-derived strains caused by the observed mutations. Truncation of ArpR caused a moderate upregulation of ArpBC locus, confirming the promiscuous function of ArpABC efflux pump as antibiotic pump and solvent pump as was previously described (35). However, other RND efflux pumps were generally downregulated in ALE-derived strains. Indeed, it has been described that a combination of different efflux pumps expression can be toxic to bacteria (36). While there are multifactorial causes of efflux pumps toxicity, including membrane composition changes and insertion machinery overload (36–38), we propose that the cause of efflux pump toxicity may be due to a high demand of proton motive force. In ALE-derived strains, F0F1 ATP syn-

these subunits, flagella and other H⁺ influx-dependent membrane transporters were severely downregulated following the moderate upregulation of ArpBC locus. Downregulation of F0F1 ATP synthase subunits may contribute to the observed fitness reduction and at the same time, required as a strategy in ALE-derived strains to overcome efflux pump toxicity in supporting the immense effort of solvent extrusion.

Truncation of putative regulator Afr in ALE-derived strains reduces expression of membrane proteins

Indel mutations were observed in a hitherto uncharacterized AraC-family transcriptional regulator (Afr), causing it to be truncated in the ALE-derived strains. In *P. putida* KT2440, a homolog of Afr encoded by PP1395 (100% identity, 100% coverage) was found to be responsible for a decrease in glycerol uptake (39), while in *P. aeruginosa* PA14, Afr homolog (63% identity, 88% coverage) encoded by PA14_38040 (PA2074 in strain PAO1) was reported to regulate the expression of RND efflux pump MexEF-OprN (40). Further characterization of Afr is underway. Since the above mentioned homologs of Afr pointed to a function regulation of transporters, truncation/deletion of Afr may contribute to the maintenance of proton motive force in ALE-derived strains.

Mutations in the *gacS/gacA* loci as a common strategy for swift phenotypic switching in Pseudomonads

Truncation of GacS protein and a SNP at *gacA* locus in ALE-derived strains resulted in the observed upregulation of its target, *rsmA* locus. Alginate biosynthesis genes, the main polysaccharide constituting Pseudomonas biofilm (29), were constitutively downregulated in ALE-derived strains. Indeed, we observed reduced biofilm formation in ALE-derived strains, which could be reversed when the mutation in *gacS* locus was complemented with wildtype sequence. In *P. aeruginosa*, biofilm dispersion can be triggered by carbon starvation and involves proton motive force dependent step(s) (41). During solvent-stress, efficient carbon catabolism and energy production is essential for the extrusion of solvent and survival of *P. putida* S12, therefore biofilm formation causing carbon starvation and oxygen depletion will be disadvantageous.

In the reverse engineering strain RE2, the deletion of *gacS* locus resulted in a significant improvement of growth parameters in the presence and absence of toluene. This mutation may have been selected for to compensate for the mutations that severely affect the

growth of ALE-derived strains, for example, the mutations at F0F1 ATP synthase loci. Similar observation was also reported in previous studies, e.g. the loss of function mutation at the *gacS/gacA* loci increased the fitness of plasmid-carrying bacterial strain (42) and improved growth characteristics and efficient root colonization (43, 44). The GacS/GacA two-component system may have a pleiotropic effect since this system regulates a large set amount of genes as a response to environmental stimuli. Additionally, *gacA/gacS* loci may constitute a commonly mutated loci which have an elevated mutation rate to allow for a swift phenotypic switching in the environmental dynamics (42–44).

General summary

In summary, ALE presents a powerful combination of mutation selection and construction of beneficial genetic variation in many different genes and regulatory regions in parallel (45, 46), for the restoration of solvent-tolerance in plasmid-cured *P. putida* S12. Through ALE, we gained insight into intrinsically promoting solvent-tolerance of *P. putida* S12. High metabolic flexibility of *P. putida* S12, e.g. ability to maintain proton motive force, indeed proved essential to incite solvent-tolerance with the availability of a solvent extrusion pump. This may very well be under the control of *gacA/gacS* loci and may involve the putative regulator Afr. Further characterization of the efficiency of solvent extrusion pumps and their impact and demand on proton motive force is required for the application of solvent-tolerant strains, especially in the bioproduction of high-value chemicals and biofuels.

References

1. Nikel PI, de Lorenzo V. *Pseudomonas putida* as a functional chassis for industrial biocatalysis: From native biochemistry to trans-metabolism. *Metab Eng* 2018; **50**: 142–155.
2. Kohlstedt M, Starck S, Barton N, Stolzenberger J, Selzer M, Mehlmann K, et al. From lignin to nylon: Cascaded chemical and biochemical conversion using metabolically engineered *Pseudomonas putida*. *Metab Eng* 2018; **47**: 279–293.
3. Wynands B, Lenzen C, Otto M, Koch F, Blank LM, Wierckx N. Metabolic engineering of *Pseudomonas taiwanensis* VLB120 with minimal genomic modifications for high-yield phenol production. *Metab Eng* 2018; **47**: 121–133.
4. Borrero-de Acuña JM, Bielecka A, Häussler S, Schobert M, Jahn M, Wittmann C, et al. Production of medium chain length polyhydroxyalkanoate in metabolic flux optimized *Pseudomonas putida*. *Microb Cell Fact* 2014; **13**: 88.
5. Poblete-Castro I, Becker J, Dohnt K, dos Santos VM, Wittmann C. Industrial biotechnology of *Pseudomonas putida* and related species. *Appl Microbiol Biotechnol* 2012; **93**: 2279–2290.
6. Verhoef S, Wierckx N, Westerhof RGM, de Winde JH, Ruijsenaars HJ. Bioproduction of p-hydroxystyrene from glucose by the solvent-tolerant bacterium *Pseudomonas putida* S12 in a two-phase water-decanol fermentation. *Appl Environ Microbiol* 2009; **75**: 931–936.
7. Meijnen JP, De Winde JH, Ruijsenaars HJ. Engineering *Pseudomonas putida* S12 for efficient utilization of D-xylose and L-arabinose. *Appl Environ Microbiol* 2008; **74**: 5031–5037.
8. Verhoef S, Ruijsenaars HJ, de Bont JAM, Wery J. Bioproduction of p-hydroxybenzoate from renewable feedstock by solvent-tolerant *Pseudomonas putida* S12. *J Biotechnol* 2007; **132**: 49–56.
9. Wierckx NJP, Ballerstedt H, de Bont JAM, Wery J. Engineering of solvent-tolerant *Pseudomonas putida* S12 for bioproduction of phenol from glucose. *Appl Environ Microbiol* 2005; **71**: 8221–8227.
10. Loeschcke A, Markert A, Wilhelm S, Wirtz A, Rosenau F, Jaeger K-E, et al. TREX: A Universal Tool for the Transfer and Expression of Biosynthetic Pathways in Bacteria. *ACS Synth Biol* 2012; **2**: 22–33.

11. Silva-Rocha R, Martínez-García E, Calles B, Chavarría M, Arce-Rodríguez A, de las Heras A, et al. The Standard European Vector Architecture (SEVA): a coherent platform for the analysis and deployment of complex prokaryotic phenotypes. *Nucleic Acids Res* 2013; **41**: D666–D675.
12. Kampers LFC, van Heck RGA, Donati S, Saccenti E, Volkens RJM, Schaap PJ, et al. In silico-guided engineering of *Pseudomonas putida* towards growth under micro-oxic conditions. *Microb Cell Fact* 2019; **18**: 179.
13. Hartmans S, Smits JP, van der Werf MJ, Volkering F, de Bont JA. Metabolism of Styrene Oxide and 2-Phenylethanol in the Styrene-Degrading *Xanthobacter* Strain 124X. *Appl Environ Microbiol* 1989; **55**: 2850–2855.
14. Koopman F, Wierckx N, de Winde JH, Ruijsenaars HJ. Efficient whole-cell biotransformation of 5-(hydroxymethyl)furfural into FDCA, 2,5-furandicarboxylic acid. *Biore-sour Technol* 2010; **101**: 6291–6296.
15. Kusumawardhani H, Hosseini R, de Winde JH. Solvent Tolerance in Bacteria: Fulfilling the Promise of the Biotech Era? *Trends Biotechnol* 2018; **36**: 1025–1039.
16. Kuepper J, Ruijsenaars HJ, Blank LM, de Winde JH, Wierckx N. Complete genome sequence of solvent-tolerant *Pseudomonas putida* S12 including megaplasmid pTTS12. *J Biotechnol* 2015; **200**: 17–18.
17. Kieboom J, Dennis JJ, de Bont JAM, Zylstra GJ. Identification and Molecular Characterization of an Efflux Pump Involved in *Pseudomonas putida* S12 Solvent Tolerance. *J Biol Chem* 1998; **273**: 85–91.
18. Kusumawardhani H, van Dijk D, Hosseini R, de Winde JH. A novel toxin-antitoxin module SlvT–SlvA regulates megaplasmid stability and incites solvent tolerance in *Pseudomonas putida* S12. *Appl Environ Microbiol* 2020; **86**: e00686-20.
19. Sprouffske K, Wagner A. Growthcurver: An R package for obtaining interpretable metrics from microbial growth curves. *BMC Bioinformatics* 2016; **17**: 172.
20. Martínez-García E, de Lorenzo V. Engineering multiple genomic deletions in Gram-negative bacteria: analysis of the multi-resistant antibiotic profile of *Pseudomonas putida* KT2440. *Environ Microbiol* 2011; **13**: 2702–2716.
21. Aparicio T, de Lorenzo V, Martínez-García E. CRISPR/Cas9-enhanced ssDNA recombineering for *Pseudomonas putida*. *Microb Biotechnol* 2019; **12**: 1076–1089.
22. Aparicio T, de Lorenzo V, Martínez-García E. CRISPR/Cas9-Based Counterselection

- Boosts Recombineering Efficiency in *Pseudomonas putida*. *Biotechnol J* 2017; **13**: e1700161.
23. Kim D, Perteza G, Trapnell C, Pimentel H, Kelley R, Salzberg SL. TopHat2: Accurate alignment of transcriptomes in the presence of insertions, deletions and gene fusions. *Genome Biol* 2013; **14**: R36.
 24. Langmead B, Salzberg SL. Fast gapped-read alignment with Bowtie 2. *Nat Methods* 2012; **9**: 357–359.
 25. O'Toole GA. Microtiter dish Biofilm formation assay. *J Vis Exp* 2010; **47**: 2437.
 26. Nadal Jimenez P, Koch G, Thompson JA, Xavier KB, Cool RH, Quax WJ. The Multiple Signaling Systems Regulating Virulence in *Pseudomonas aeruginosa*. *Microbiol Mol Biol Rev* 2012; **76**: 46–65.
 27. Kieboom J, de Bont JAM. Identification and molecular characterization of an efflux system involved in *Pseudomonas putida* S12 multidrug resistance. *Microbiology* 2001; **147**: 43–51.
 28. Wijte D, van Baar BLM, Heck AJR, Altelaar AFM. Probing the proteome response to toluene exposure in the solvent tolerant *Pseudomonas putida* S12. *J Proteome Res* 2011; **10**: 394–403.
 29. Whitney JC, Whitfield GB, Marmont LS, Yip P, Neculai AM, Lobsanov YD, et al. Dimeric c-di-GMP is required for post-translational regulation of alginate production in *Pseudomonas aeruginosa*. *J Biol Chem* 2015; **290**: 12451–12462.
 30. Hews CL, Cho T, Rowley G, Raivio TL. Maintaining Integrity Under Stress: Envelope Stress Response Regulation of Pathogenesis in Gram-Negative Bacteria. *Front Cell Infect Microbiol* 2019; **9**: 313.
 31. Yorgey P, Rahme LG, Tan MW, Ausubel FM. The roles of mucD and alginate in the virulence of *Pseudomonas aeruginosa* in plants, nematodes and mice. *Mol Microbiol* 2001; **41**: 1063–1076.
 32. Molina-Santiago C, Udaondo Z, Gómez-Lozano M, Molin S, Ramos JL. Global transcriptional response of solvent-sensitive and solvent-tolerant *Pseudomonas putida* strains exposed to toluene. *Environ Microbiol* 2017; **19**: 645–658.
 33. Garikipati SVBJ, Mclver AM, Peeples TL. Whole-Cell Biocatalysis for 1-Naphthol Production in Liquid-Liquid Biphasic Systems. *Appl Environ Microbiol* 2009; **75**: 6545–6552.

34. Janardhan Garikipati SVB, Peeples TL. Solvent resistance pumps of *Pseudomonas putida* S12: Applications in 1-naphthol production and biocatalyst engineering. *J Biotechnol* 2015; **210**: 91–99.
35. Rojas A, Duque E, Mosqueda G, Golden G, Hurtado A, Ramos JL, et al. Three efflux pumps are required to provide efficient tolerance to toluene in *Pseudomonas putida* DOT-T1E. *J Bacteriol* 2001; **183**: 3967–3973.
36. Turner WJ, Dunlop MJ. Trade-Offs in Improving Biofuel Tolerance Using Combinations of Efflux Pumps. *ACS Synth Biol* 2015; **4**: 1056–1063.
37. Alsaker K V, Paredes C, Papoutsakis ET. Metabolite stress and tolerance in the production of biofuels and chemicals: gene-expression-based systems analysis of butanol, butyrate, and acetate stresses in the anaerobe *Clostridium acetobutylicum*. *Biotechnol Bioeng* 2010; **105**: 1131–1147.
38. Wagner S, Baarst L, Ytterberg AJ, Klussmerer A, Wagner CS, Nord O, et al. Consequences of membrane protein overexpression in *Escherichia coli*. *Mol Cell Proteomics* 2007; **6**: 1527–1550.
39. Beckers V, Poblete-Castro I, Tomasch J, Wittmann C. Integrated analysis of gene expression and metabolic fluxes in PHA-producing *Pseudomonas putida* grown on glycerol. *Microb Cell Fact* 2016; **15**: 73.
40. Juarez P, Jeannot K, Plésiat P, Llanes C. Toxic Electrophiles Induce Expression of the Multidrug Efflux Pump MexEF-OprN in *Pseudomonas aeruginosa* through a Novel Transcriptional Regulator, CmrA. *Antimicrob Agents Chemother* 2017; **61**: e00585-17.
41. Huynh TT, McDougald D, Klebensberger J, Al Qarni B, Barraud N, Rice SA, et al. Glucose starvation-induced dispersal of *Pseudomonas aeruginosa* biofilms is camp and energy dependent. *PLoS One* 2012; **7**: e42874.
42. Harrison E, Guymer D, Spiers AJ, Paterson S, Brockhurst MA. Parallel Compensatory Evolution Stabilizes Plasmids across the Parasitism-Mutualism Continuum. *Curr Biol* 2015; **25**: 2034–2039.
43. Van Den Broek D, Bloemberg G V., Lugtenberg B. The role of phenotypic variation in rhizosphere *Pseudomonas* bacteria. *Environ Microbiol* 2005; **7**: 1686–1697.
44. Seaton SC, Silby MW, Levy SB. Pleiotropic effects of GacA on *Pseudomonas fluorescens* Pf0-1 in vitro and in soil. *Appl Environ Microbiol* 2013; **79**: 5405–5410.

45. Dragosits M, Mattanovich D. Adaptive laboratory evolution -- principles and applications for biotechnology. *Microb Cell Fact* 2013; **12**: 64.
46. Portnoy VA, Bezdán D, Zengler K. Adaptive laboratory evolution — harnessing the power of biology for metabolic engineering. *Curr Opin Biotechnol* 2011; **22**: 590–594.
47. Hartmans S, van der Werf MJ, de Bont JA. Bacterial degradation of styrene involving a novel flavin adenine dinucleotide-dependent styrene monooxygenase. *Appl Environ Microbiol* 1990; **56**: 1347–1351.

Supplementary Materials

Table 5.S1. Strains and plasmids used in this paper

Strain	Characteristics	Ref.
<i>P. putida</i> S12	Wild type <i>P. putida</i> S12 (ATCC 700801), harboring megaplasmid pTTS12, solvent-tolerant strain	(47)
<i>P. putida</i> S12d (S12-06/ S12-10/ S12-22)	<i>P. putida</i> S12 ΔpTTS12, non-solvent-tolerant strains	(18)
<i>P. putida</i> S12e (S12-06e30/ S12-10e35/ S12-22e30)	ALE-derived <i>P. putida</i> S12 ΔpTTS12, solvent-tolerant strain	This paper
<i>P. putida</i> S12d ΔarpR	<i>P. putida</i> S12 ΔpTTS12 ΔRPPX_14650	This paper
<i>P. putida</i> S12d Δafr	<i>P. putida</i> S12 ΔpTTS12 ΔRPPX_14685	This paper
<i>P. putida</i> S12d ΔgacA	<i>P. putida</i> S12 ΔpTTS12 ΔRPPX_00635	This paper
<i>P. putida</i> S12d ΔgacS	<i>P. putida</i> S12 ΔpTTS12 ΔRPPX_15700	This paper
<i>P. putida</i> S12e arpR-wt	ALE-derived <i>P. putida</i> S12 ΔpTTS12 RPPX_14650-wt	This paper
<i>P. putida</i> S12e afr-wt	ALE-derived <i>P. putida</i> S12 ΔpTTS12 RPPX_14685-wt	This paper
<i>P. putida</i> S12e gacS-wt	ALE-derived <i>P. putida</i> S12 ΔpTTS12 RPPX_15700-wt	This paper
<i>P. putida</i> S12e rpoB ⁻ -wt	ALE-derived <i>P. putida</i> S12 ΔpTTS12 RPPX_06985-wt	This paper
<i>P. putida</i> S12e ATP-wt	ALE-derived <i>P. putida</i> S12 ΔpTTS12 RPPX_09480-09510-wt	This paper
<i>P. putida</i> S12 ΔlapA	<i>P. putida</i> S12 ΔRPPX_08475	This paper
<i>P. putida</i> S12 Δflg	<i>P. putida</i> S12 ΔRPPX_02040-02125	This paper
<i>P. putida</i> S12-RE1	<i>P. putida</i> S12-10 (ΔpTTS12) ΔarpR	This paper
<i>P. putida</i> S12-RE2	<i>P. putida</i> S12-10 (ΔpTTS12) ΔarpR; ΔgacS	This paper
<i>P. putida</i> S12-RE3	<i>P. putida</i> S12-10 (ΔpTTS12) ΔarpR; ΔgacS; atpα (R165C)	This paper
<i>P. putida</i> S12-RE4	<i>P. putida</i> S12-10 (ΔpTTS12) ΔarpR; ΔgacS; atpα (R165C); Δafr	This paper
<i>P. putida</i> S12-RE5	<i>P. putida</i> S12-10 (ΔpTTS12) ΔarpR; ΔgacS; atpα (R165C); Δafr; rpoB ['] (D622G)	This paper
<i>E. coli</i> WM3064	<i>thrB1004 pro thi rpsL hsdS lacZ</i> ΔM15 RP4-1360 Δ(<i>araBAD</i>)567 Δ <i>dapA1341</i> ::[erm pir]	William Metcalf
Plasmid	Description	Ref.
pEMG	Km ^R , Ap ^R , <i>ori</i> R6K, <i>lacZ</i> α MCS flanked by two I-SceI sites	(20)
pEMG-ΔarpR	pEMG plasmid for constructing <i>P. putida</i> S12d Δafr	This paper
pEMG-Δafr	pEMG plasmid for constructing <i>P. putida</i> S12d Δafr	This paper

Plasmid	Description	Ref.
pEMG- $\Delta gacA$	pEMG plasmid for constructing <i>P. putida</i> S12d $\Delta gacA$	This paper
pEMG- $\Delta gacS$	pEMG plasmid for constructing <i>P. putida</i> S12d $\Delta gacS$	This paper
pEMG- $\Delta lapA$	pEMG plasmid for constructing <i>P. putida</i> S12 $\Delta lapA$	This paper
pEMG- Δflg	pEMG plasmid for constructing <i>P. putida</i> S12 Δflg	This paper
pEMG-c- <i>arpR</i>	pEMG plasmid for constructing <i>P. putida</i> S12e <i>arpR</i> -wt	This paper
pEMG-c- <i>afr</i>	pEMG plasmid for constructing <i>P. putida</i> S12e <i>afr</i> -wt	This paper
pEMG-c- <i>gacS</i>	pEMG plasmid for constructing <i>P. putida</i> S12e <i>gacS</i> -wt	This paper
pEMG-c- <i>rpoB'</i>	pEMG plasmid for constructing <i>P. putida</i> S12e <i>rpoB'</i> -wt	This paper
pEMG-c-ATP	pEMG plasmid for constructing <i>P. putida</i> S12e ATP-wt	This paper
pSW-2	Gm ^R , <i>ori</i> RK2, <i>xyIS</i> , Pm ® I-sceI	(20)
p421-cas9	Cas9 and tracrRNA; <i>oriV</i> RK2; Sm ^R /Sp ^R	(22)
p658-ssr	<i>xyIS</i> -Pm → <i>ssr</i> , <i>oriV</i> RSF1010; Gm ^R	(22)
p2316	SEVA CRISPR array; <i>oriV</i> pBBR1; Km ^R	(21)
p2316-ATPsyn	pSEVA2316 derivative containing the ATP synthase spacer	This paper
p2316- <i>rpoB'</i> -622	pSEVA2316 derivative containing the <i>rpoB'</i> spacer (substitution of amino acid D622G)	This paper

Table 5.S2. Oligos used in this study

Oligos	Sequence	Purpose
Afr_test_F	gaaacgaccatgtaatgc	PCR and sanger sequencing of mutated region within RPPX_14685
Afr_test_R	gaggaaagccatcatgac	PCR and sanger sequencing of mutated region within RPPX_14685
ArpR_test_F	gtcgaaccaaagaagaag	PCR and sanger sequencing of mutated region within RPPX_14650
ArpR_test_R	gctgaagactacgcaatc	PCR and sanger sequencing of mutated region within RPPX_14650
ATP_test_F	ggttattcgctacaactc	PCR and sanger sequencing of mutated region in the intergenic region of RPPX_09485-09490
ATP_test_R	gaagatcaacaggaagatc	PCR and sanger sequencing of mutated region in the intergenic region of RPPX_09485-09490
ATPa_test_F	aaaggtcctctgggtaac	PCR and sanger sequencing of mutated region within RPPX_09510
ATPa_test_R	gacagcaacataaacacag	PCR and sanger sequencing of mutated region within RPPX_09510
GacA_test_F	atctcgggctgatatag	PCR and sanger sequencing of mutated region within RPPX_000635
GacA_test_R	gttgctgatgatgtg	PCR and sanger sequencing of mutated region within RPPX_000635
GacS_test_F	cgacagctcgatctctac	PCR and sanger sequencing of mutated region within RPPX_15700
GacS_test_R	caactggagagaattgcc	PCR and sanger sequencing of mutated region within RPPX_15700
rpoB1_test_45_F	acttcaacgccgcacttc	PCR and sanger sequencing of mutated region within RPPX_06985, for the mutation N45S
rpoB1_test_45_R	ctgaaagacctactgaattgc	PCR and sanger sequencing of mutated region within RPPX_06985, for the mutation N45S
rpoB1_test_410_F	ttacctcgatcagtagcg	PCR and sanger sequencing of mutated region within RPPX_06985, for the mutation D622G
rpoB1_test_410_R	ggtaagcgtgttgactactcc	PCR and sanger sequencing of mutated region within RPPX_06985, for the mutation D622G
rpoB1_test_622_F	gtactggctctcgatttc	PCR and sanger sequencing of mutated region within RPPX_06985, for the mutation D410E
rpoB1_test_622_R	ttgactgggtctgtactacat	PCR and sanger sequencing of mutated region within RPPX_06985, for the mutation D410E
Flg_test_F	catacatttcgcgtagac	PCR and sanger sequencing of the knocked-out flagella gene cluster

Oligos	Sequence	Purpose
Flg_test_F	agaataagcagctacgtggttc	PCR and sanger sequencing of the knocked-out flagella gene cluster
KO_TS1_ArpR_F	cgggcgaattctcttcttcttacagccact	ΔRPPX_14650
KO_TS1_ArpR_R	aacagatcgacactgtcagcttgtagaaggccctttc	ΔRPPX_14650
KO_TS2_ArpR_F	gaaagggccttctacaagctgacagtgatgatctgtt	ΔRPPX_14650
KO_TS2_ArpR_R	cggactctagactacaaccacagatcctg	ΔRPPX_14650
KO_TS1_Afr_F	cctcaggatccctcagtcgaaggtatgcaagtcca	ΔRPPX_14685
KO_TS1_Afr_R	Ttcttcacctttatgaattcccatgatcatgatggcttc ctctgctgaccg	ΔRPPX_14685
KO_TS2_Afr_F	Cgcacggcatggatgaactctacaataaagct- caa cattcgctgcaccg	ΔRPPX_14685
KO_TS2_Afr_R	ggcgatctagaccaacctgtgtataccggcaacct	ΔRPPX_14685
KO_TS1_GacA_F	tagtagctactctcgactg	ΔRPPX_00635
KO_TS1_GacA_R	ctcatgtccaagtcttt	ΔRPPX_00635
KO_TS2_GacA_F	accactaagaccctaataca	ΔRPPX_00635
KO_TS2_GacA_R	catagtgaaatccatagctttac	ΔRPPX_00635
KO_TS1_GacS_F	gagttcgctcattgatgaag	ΔRPPX_15700
KO_TS1_GacS_R	ctgacatgctgagatgct	ΔRPPX_15700
KO_TS2_GacS_F	atccttgagctgattgac	ΔRPPX_15700
KO_TS2_GacS_R	ggtagctatttcacctgg	ΔRPPX_15700
KO_TS1_lapA_F	agattgaattcaagtacaacctataactgtcc	knocking-out lapA/adhesin, negative control for biofilm assay
KO_TS1_lapA_R	gtggcgtaatctgtttataatcatcatccacaacaag	knocking-out lapA/adhesin, negative control for biofilm assay
KO_TS2_lapA_F	ctgttggtgatgatgattataaacgattacgccac	knocking-out lapA/adhesin, negative control for biofilm assay
KO_TS2_lapA_R	gggcatctagagtgacttatcgaaggtgac	knocking-out lapA/adhesin, negative control for biofilm assay
KO_TS1_flg_F	ggcagggatccggaagaaattcacctaaaagc	knocking-out flagella gene cluster, negative control for swimming motility assay
KO_TS1_flg_R	ctatacctgtctcaacgaaattgaagagatgatg- cagatcaatc	knocking-out flagella gene cluster, negative control for swimming motility assay
KO_TS2_flg_F	gattgatctgcatcatctctcaatttcggtgagcaag- gtag	knocking-out flagella gene cluster, negative control for swimming motility assay
KO_TS2_flg_R	cgtgttctagaggaatgtgctgatctatttctc	knocking-out flagella gene cluster, negative control for swimming motility assay
c_Afr_F	gcaatgaattcatctgtgcaaaaacctgta	complementation of RPPX_14685 to the wild-type sequence in the evolved strains
c_Afr_R	aggggtctagaacaatctccttgaagcag	complementation of RPPX_14685 to the wild-type sequence in the evolved strains
c_ArpR_F	ccttcaattccgaagagcgaccgatcgg	complementation of RPPX_14650 to the wild-type sequence in the evolved strains
c_ArpR_R	ttcttctagactccagtcatttcgctgacc	complementation of RPPX_14650 to the wild-type sequence in the evolved strains

Oligos	Sequence	Purpose
c_ATPa_F	cgaaagaattcgaagcattgaaatcttgag	complementation of RPPX_09510 to the wild-type sequence in the evolved strains
c_ATPa_R	tgatgtctagaatcttactcgaatctcttt	complementation of RPPX_09510 to the wild-type sequence in the evolved strains
c_GacA_F	gcgctgaattcaagacttgggacatgag	complementation of RPPX_00635 to the wild-type sequence in the evolved strains
c_GacA_R	gaggtggatccttgattagggtcttagtggt	complementation of RPPX_00635 to the wild-type sequence in the evolved strains
c_GacS_F	cagccgaattcaagcttctctgatcgtag	complementation of RPPX_15700 to the wild-type in the evolved strains
c_GacS_R	ggcaatctagaataaacactactaaagagatgc	complementation of RPPX_15700 to the wild-type in the evolved strains
c_ATP_F	gcactggatccacaacttaaggaatccgtat	complementation of RPPX_09485-09490 to the wild-type sequence in the evolved strains
c_ATP_R	gtcagtctagacaagtggtgctggatag	complementation of RPPX_09485-09490 to the wild-type sequence in the evolved strains
c_rpoB1_F	ccaaggatccggtagacaaaagtctaaagaggat	complementation of RPPX_06985 to the wild-type sequence in the evolved strains
c_rpoB1_R	aggagtctagacctgaaagacctactgaat	complementation of RPPX_06985 to the wild-type sequence in the evolved strains
cr-rpoBWT-622-1-S	aaacagtaagcgaaccgggtgtacatcagctggtg	spacer fragment for introducing D622G point mutation at RPPX_06985
cr-rpoBWT-622-1-AS	aaaacaccagctgatgtacaccggttctgcttact	spacer fragment for introducing D622G point mutation at RPPX_06985
RpoB-622e-1	Gaaatggtcagtagcgaaccgggtgtacatcagctggccggcgaagataacgggtctcttcagac-caaccacgcggtag	repair fragment for introducing D622G point mutation at RPPX_06985
cr-ATPWT-1-S	aaacatctgacggtcgccaatgatcagctcacgcg	spacer fragment for introducing R165C point mutation at RPPX_09510
cr-ATPWT-1-AS	aaaacgcgtgagctgatcattggcgaccgtcagat	spacer fragment for introducing R165C point mutation at RPPX_09510
ATP-09510e-1	Gtctgccgatctgacggtcgccaatgatcagctcactggccacggccgacagggatcatggcgtc-gacggattgtaaccag	repair fragment for introducing R165C point mutation at RPPX_09510

Table 5.S3. Growth parameters of ALE-derived and reverse engineering strains

Strains	Media	Lag time (minutes)	μ_{\max} (h ⁻¹)		maxOD	
			μ_{\max}	sd	maxOD	sd
ALE						
S12	LB	180	1.18	0.090	0.90	0.038
S12e30		180	1.02*	0.021	0.87	0.027
S12-06		180	1.14	0.026	0.88	0.048
S12-06e30		180	0.80*	0.029	0.82*	0.036
S12-10		180	1.15	0.038	0.89	0.039
S12-10e35		180	0.78*	0.030	0.83*	0.032
S12-22		195	1.07	0.037	0.88	0.045
S12-22e30		180	0.79*	0.018	0.82*	0.034
S12	MM + citrate	180	1.02	0.105	0.88	0.064
S12e30		180	1.05	0.044	0.86	0.027
S12-06		165	1.01	0.095	0.83	0.027
S12-06e30		225	0.48*	0.058	0.54*	0.130
S12-10		165	1.02	0.141	0.83	0.032
S12-10e35		255	0.47*	0.044	0.37*	0.145
S12-22		165	0.99	0.078	0.84	0.019
S12-22e30		240	0.41*	0.049	0.30*	0.115
S12	MM + glucose	150	0.89	0.072	1.00	0.024
S12e30		150	1.06*	0.021	0.99	0.009
S12-06		150	0.95	0.027	1.02	0.033
S12-06e30		180	0.71*	0.028	0.66*	0.074
S12-10		150	0.97	0.058	1.03	0.033
S12-10e35		195	0.70*	0.032	0.70*	0.199
S12-22		150	0.94	0.033	1.02	0.022
S12-22e30		210	0.73*	0.019	0.62*	0.161
S12	MM + glycerol	195	1.16	0.119	1.04	0.006
S12e30		195	1.04	0.010	0.89*	0.046
S12-06		195	1.11	0.138	1.09	0.051
S12-06e30		255	0.54*	0.044	0.82*	0.010
S12-10		180	1.11	0.159	1.08	0.046
S12-10e35		315	0.50*	0.011	0.79*	0.031
S12-22		195	1.17	0.119	1.10	0.044
S12-22e30		300	0.52*	0.029	0.80*	0.011

Strains	Media	Lag time (minutes)	μ_{\max} (h ⁻¹)		maxOD	
			μ_{\max}	sd	maxOD	sd
Reverse engineering						
RE1	LB	195	0.88	0.013	0.93	0.0498
RE2		105**	0.96**	0.017	0.96	0.0468
RE3		135*	0.88*	0.035	1.07	0.1016
RE4		135	0.89	0.035	1.07	0.0985
RE5		135	0.94	0.029	1.04	0.0937
RE1	MM + citrate	195	1.02	0.048	0.85	0.0605
RE2		150**	0.97	0.025	0.94	0.0460
RE3		240*	0.54*	0.106	0.51*	0.1681
RE4		240	0.57	0.096	0.40	0.0698
RE5		240	0.49	0.067	0.44	0.1328
RE1	MM + glucose	120	0.98	0.031	1.02	0.0326
RE2		120	1.04	0.018	1.00	0.0399
RE3		165*	0.84*	0.077	0.64*	0.0917
RE4		165	0.78	0.083	0.63	0.1286
RE5		165	0.93	0.140	0.59	0.1101
RE1	MM + glycerol	150	1.10	0.044	1.00	0.0958
RE2		120**	1.14	0.072	0.99	0.1264
RE3		180*	0.78*	0.101	1.06	0.2613
RE4		180	0.79	0.098	1.02	0.2867
RE5		180	0.87	0.098	1.10	0.2124

*) significant reduction of growth parameter in comparison to its parent strain

**) significant improvement of growth parameter in comparison to its parent strain

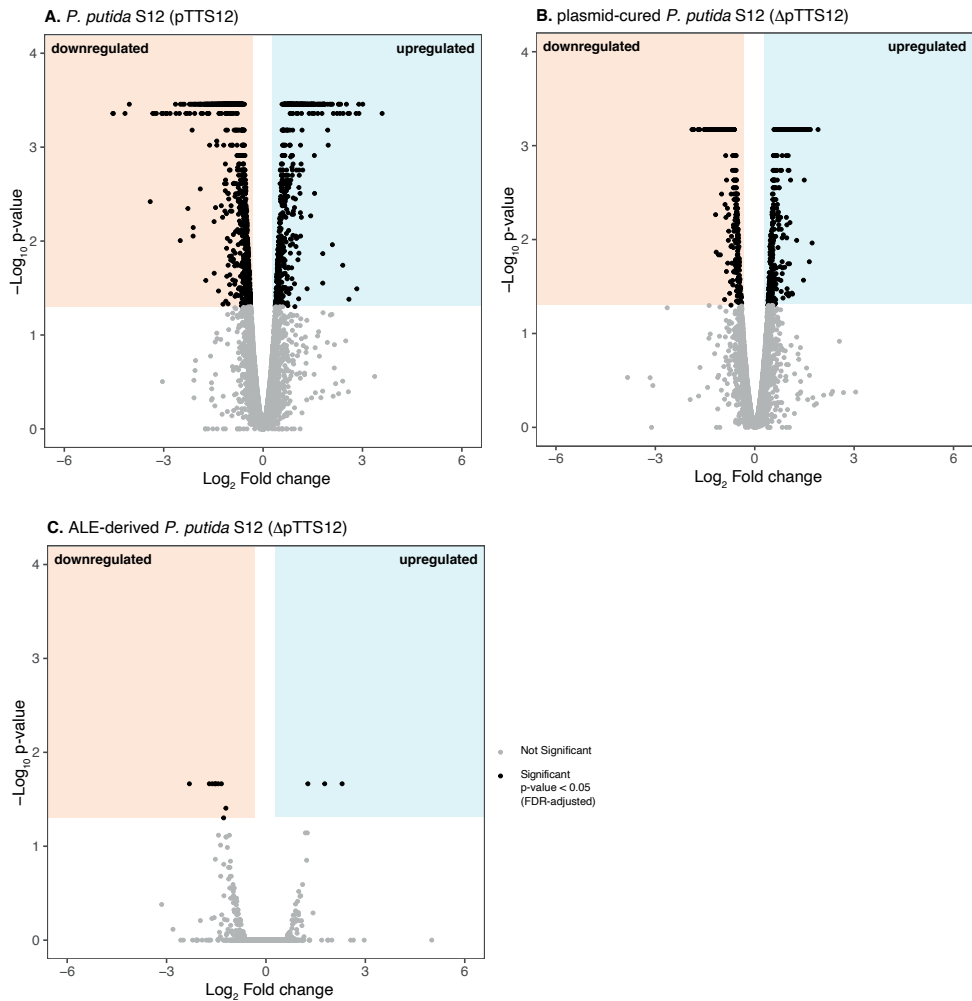


Fig. 5.S1. Volcano plot of differential gene expression in *P. putida* S12, S12 Δ pTTS12, and ALE-derived strains in the presence of toluene.

Control strains were refers on LB medium for 2 hours before sampling and sample strains were grown on LB medium with 0.1% (vol/vol) toluene for 2 hours before sampling. Blue area indicates the significantly upregulated genes and beige area indicates the significantly downregulated genes (cut-off: Log_2 Fold Change ≥ 1 for up-regulated genes or ≤ 1 for down-regulated genes and FDR-adjusted p-value ≤ 0.05).